

# Factors Affecting the Solid-State Polymerization of 1,4-Bis(1,3-octadecadiynyl)benzene to a Polydiacetylene

William S. Price,\* Naoto Kikuchi, Hiro Matsuda, and Kikuko Hayamizu

National Institute of Materials and Chemical Research,  
1-1 Higashi, Tsukuba, Ibaraki 305, Japan

Shuji Okada and Hachiro Nakanishi

Institute for Chemical Reaction Science, Tohoku University,  
2-1-1 Katahira, Aoba-ku, Sendai 980-77, Japan

Received February 13, 1995; Revised Manuscript Received May 5, 1995\*

**ABSTRACT:** In an attempt to produce a polydiacetylene (PDA) with larger third order nonlinear optical properties, the polymer precursor, 1,4-bis(1,3-octadecadiynyl)benzene, was synthesized. It was found, however, that neither thermal treatment (up to 343 K) nor  $\gamma$ -ray irradiation at above 300 K was able to promote solid-state polymerization. A detailed analysis of the molecular motion was conducted using differential scanning calorimetry, solid-state cross-polarization magic-angle-spinning  $^{13}\text{C}$ , and solid-state  $^2\text{H}$  NMR and solution-state  $^{13}\text{C}$  NMR. It was found that below 300 K the monomer undergoes small-amplitude motions only. Above 300 K the sp-bonded phenyl ring undergoes  $\pi$  flips around the long axis of the molecule at an intermediate rate with respect to the NMR time scale ( $< 2 \times 10^{-5} \text{ Hz}^{-1}$ ) with an activation energy of  $60 \pm 1 \text{ kJ mol}^{-1}$ . The poor polymerization above 300 K was attributed to the monomers being unable to obtain the proper alignment with respect to each other necessary for the polymerization process. The results of this study lead to the successful polymerization of the monomer by using  $\gamma$ -ray irradiation but at 273 K. The structure of the polymer was determined using solid-state  $^{13}\text{C}$  NMR.

## Introduction

Non-linear optical materials are extremely important in opto-electronic and photonic applications.<sup>1</sup> Organic nonlinear optical media are of particular interest for a number of reasons including their ease of fabrication, tailorability, and fast nonlinear optical response times. Of the organic media, polydiacetylenes (PDA's) are one of the best candidates<sup>2</sup> and have been the subject of a number of recent reviews.<sup>3,4</sup> Their unique one-dimensional  $\pi$ -conjugated structure and third-order nonlinear optical properties have been extensively investigated.<sup>2,5–7</sup> PDA's are synthesized by topochemical solid-state polymerization.<sup>8</sup>

In our recent work we have been attempting to increase the third-order susceptibility of PDA-based nonlinear optical polymers by synthesizing PDA's with greater numbers of  $\pi$  electrons per repeating unit through  $\pi$ -conjugation.<sup>9–14</sup> It was thought that the compound 1,4-bis(1,3-octadecadiynyl)benzene (Bis(14–2A)B; where A represents acetylene, B represents the phenyl ring in a *p*-phenylene group, and 14 refers to the 14 carbon alkyl chain; see Figure 1) would, if polymerized, form an excellent nonlinear optical polymer. However, it was found (*vide infra*) that neither thermal treatment nor  $\gamma$ -irradiation above 300 K would induce solid-state polymerization. In our previous studies it was found that some monomers polymerized much more easily than others. It has been noted that monomer side groups have a strong influence on the molecular organization and polymerization behavior in the solid state.<sup>15</sup> Most polymerizable PDA's have methylene groups next to the diacetylene moiety. However, to obtain PDA's with aromatic substituents directly bound to the main chain is not easy. For example, diphenyldiacetylenes and dicarbazolyldiacetylenes<sup>16</sup> are not polymerizable by the 1,4-addition mechanism, and

several substituted diphenyldiacetylenes give polymers only in low yield. Depending upon the chemical nature of the side groups, a number of crystalline phases may be present with different conformations of the side groups. Whether solid-state polymerization will occur in a particular crystalline phase depends upon the intermolecular spacings and precise arrangement of the adjacent diacetylene functionalities.<sup>15,17</sup> Previous studies have shown that, in solid-state polymerizable diacetylene crystals, the molecules are piled up along the translation axis of about 5 Å with an angle of inclination of 45° to form an inclined stack so that the atoms that form a bond in the 1,4-addition are in close proximity.<sup>15,17</sup> However, with aromatic substituted diacetylenes (2A's) the molecules tend to form simple plane-to-plane parallel stacks along the shorter translation axis, with inclination angles being compound dependent. Because of strong interplanar interactions between the aromatic rings, the acetylene terminal carbons in adjacent 2A monomers are not sufficiently close to allow polymerization. Following several empirical rules for obtaining polymerizable stacks for the diarylbutadiynes, we successfully prepared several PDA's substituted directly by aromatic rings.<sup>18</sup> Substituents for producing  $\pi$ -conjugation between the polymer backbone and side chains have been expanded from aromatic ring groups to acetylenic groups. Work in our laboratory has shown that the monomers 15,17-dotriacontadiyne (14–2A), 10,12,14-nonacosatriyonic acid (14–3A–8C, where 8C represents an 8-carbon aliphatic chain terminated by a carboxylic acid group), and 15,17,19,21-hexatriacontatetrayne (14–4A) are polymerizable, with the 14–4A monomer polymerizing with near 100% efficiency.<sup>19</sup> As mentioned above, PDA's having methylene groups often show solid-state polymerizability, and it is thought that the van der Waals forces between the bent methylenes prevents parallel stack formation. Perhaps such a mechanism would still hold even if there was a methylene group on only one side. This led to the idea of using unsymmetrical 2A with a methylene group on one

\* Abstract published in *Advance ACS Abstracts*, June 15, 1995.

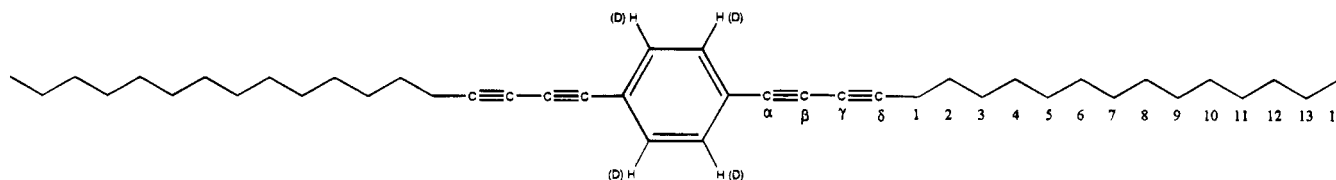


**Figure 1.** Structure of the compound Bis(14-2A)B.  $^2\text{H}$  NMR measurements were performed on a sample containing a selectively  $^2\text{H}$ -labeled phenyl ring as indicated in the figure.

side and an aromatic on the other<sup>20</sup> and unsymmetrical 4A (13-(4-butyl-2,3,5,6-tetrafluorophenyl)-6,8,10,12-tridecatetraynyl *N*-(butoxycarbonylmethyl) carbamate).<sup>21</sup> Amphiphilic 2A's are polymerizable in Langmuir-Blodgett films due to the anchor void effect whereby the monomer is anchored at the hydrophilic end. van der Waals forces between the alkyl chains result in the 2A moieties becoming inclined until they reach the proper van der Waals distance, resulting in a polymerizable stack.<sup>22</sup>

In an effort to understand the poor polymerizability of the Bis(14-2A)B monomer, solid-state cross-polarization magic-angle-spinning (CP-MAS) spectra were recorded for a number of temperatures ranging from 273 to 343 K. It was noted that the aromatic CH carbon resonances were not able to be observed at 298 K (*vide infra*). The effect is consistent with increased molecular motion of the phenyl ring moiety.<sup>23,24</sup> To better understand the molecular dynamics of the monomer and especially the phenyl ring moiety a  $^2\text{H}$ -labeled Bis(14-2A)B monomer was synthesized (see Figure 1) so that solid-state  $^2\text{H}$  NMR powder spectra could be observed.  $^2\text{H}$  NMR is a powerful technique for determining both the type and rate of motion of molecules in the solid state (e.g., Rice et al.<sup>25</sup> and Cholli et al.<sup>26</sup>). In the present work the motion of the monomer and the effects of both thermal and  $\gamma$ -irradiation for initiating solid-state polymerization were investigated using differential scanning calorimetry (DSC), solid-state  $^{13}\text{C}$  NMR and  $^2\text{H}$  NMR techniques. Changes noted in the solid-state  $^{13}\text{C}$  NMR, and  $^2\text{H}$  NMR spectra were found to correlate with a phase change observed in the calorimetry measurement. From the results of this investigation it was found that the difficulties in polymerizing this compound at 298 K and above were due to the loss of alignment of the monomer molecules. This loss of alignment coincided with the onset of rotational motion of the phenyl ring. Further, with this new found understanding of the monomer molecular dynamics, a successful procedure to polymerize the monomer at low temperature using  $\gamma$ -ray irradiation was devised. The resulting polymer was then examined using solid-state  $^{13}\text{C}$  CP-MAS NMR. Solid-state  $^{13}\text{C}$  NMR spectroscopy was used to characterize the resulting polymer and also confirmed that the polymerization occurred via the 1,4-addition mechanism.

## Experimental Section

**Synthesis of Compounds.** 1,4-Bis(1,3-octadecadiynyl)-benzene was prepared by the palladium(0)-catalyzed coupling reaction<sup>27,28</sup> of 1,3-octadecadiyne and 1,4-diiodobenzene as follows: To a solution of 1,3-octadecadiyne<sup>11</sup> (1.033 g, 4.2 mmol) and 1,4-diiodobenzene (660 mg, 2 mmol) in triethylamine (30 mL) were added at ambient temperature under an argon atmosphere bis(triphenylphosphine)palladium(II) chloride (28 mg) and copper(I) chloride (8 mg). After this was stirred overnight, the solvent was removed under reduced pressure, and the residue was purified by column chromatography (silica gel, hexane) and recrystallized from hexane to give 493 mg (44%) of 1,4-bis(1,3-octadecadiynyl)benzene.

Mp: 376–377.5 K. IR (KBr): 2955, 2921, 2849, 2422 (weak), 1470, 839, 830, 722, 546  $\text{cm}^{-1}$ .  $^1\text{H}$  NMR ( $\text{CDCl}_3$ ):  $\delta$  0.88 (6H, t,  $J$  = 6.6 Hz), 1.15–1.35 (40 H, m), 1.40 (4H, m), 1.55 (4H, m), 2.36 (4H, t,  $J$  = 6.9 Hz), 7.39 (4H, s).  $^{13}\text{C}$  NMR ( $\text{CDCl}_3$ )  $\delta$  = 14.14, 19.65, 22.70, 28.20, 28.88, 29.09, 29.37, 29.48, 29.62, 29.66 (four peaks overlapped), 31.93, 64.93, 74.06, 76.73, 86.33, 122.50, 132.35. Found: C, 88.93; H, 11.30. Calcd for  $\text{C}_{42}\text{H}_{62}$ : C, 88.98; H, 11.02. 1-Iodo-4-(1,3-octadecadiynyl)benzene was also obtained as a byproduct.

The derivative containing a deuterated phenyl group, i.e., 1,4-bis(1,3-octadecadiynyl)benzene-2,3,5,6- $d_4$ , was synthesized by the same procedure but using 1,4-diiodobenzene- $d_4$  instead of 1,4-diiodobenzene. Mp: 375–376.5 K. IR (KBr): 2955, 2923, 2849, 2236 (weak), 2149 (weak), 1468, 1420, 1321, 1289, 862, 818, 722, 505, 482, 444  $\text{cm}^{-1}$ . Found: C, 88.63; H and D, 11.31. Calcd for  $\text{C}_{42}\text{H}_{58}\text{D}_4$ : C, 88.35; H and D, 11.65. Deuterated diiodobenzene was obtained by iodation<sup>29</sup> of benzene- $d_6$  (Merck Uvasol, isotopic purity of more than 99.8%). The deuterated monomer was used only for the solid-state  $^2\text{H}$  NMR experiments. The specificity and degree of deuteration of the monomer was checked by solution-state  $^{13}\text{C}$  NMR of a sample of labeled monomer (7.3 mg) in 0.6 mL of  $\text{CDCl}_3$ . Undeuterated monomer was not detected.

**DSC.** Differential scanning calorimetry measurements were performed using a DSC 8230 calorimeter (Rigaku Co., Tokyo). Measurements were performed on a 1 mg sample at a heating rate of 5 K  $\text{min}^{-1}$ .

**NMR.** Solid-state  $^{13}\text{C}$  CP-MAS and  $^{13}\text{C}$  dipole-dephasing CP-MAS (CP-MAS/DD) spectra were acquired using a 7 mm probe on a JEOL GSH-200 spectrometer operating at 50.23 MHz. The CP-MAS spectra were acquired in the presence of proton-decoupling. Typical acquisition parameters were a MAS speed of 4.5 kHz and a  $^1\text{H}$   $\pi/2$  pulse width of 4.2  $\mu\text{s}$ . Since the molecules were assumed to be quite mobile, a relatively long CP time of 3 ms was used to improve the signal-to-noise ratio. The  $\text{CH}_2$  peak (29.5 ppm) of external adamantane was used as the  $^{13}\text{C}$  chemical shift reference.  $^{13}\text{C}$  spin-lattice relaxation times were measured using CP.<sup>30</sup>

Solid-state  $^2\text{H}$  NMR spectra were acquired using a 5 mm probe on a Bruker MSL-400 spectrometer operating at 61.4 MHz using the quadrupole echo pulse sequence (i.e.,  $\pi/2x - \tau - \pi/2y - \tau - \text{Acq.}$ ). Typical acquisition parameters were a  $\pi/2$  pulse width of 2.9  $\mu\text{s}$ , a  $\tau$  delay time of 20 ms, and a spectral width of 2.5 MHz digitized into 2 K data points. At each temperature the spin-lattice relaxation time ( $T_1$ ) of the slowest relaxing component in the spectrum was approximately determined from the null-point in inversion-recovery experiments. The preacquisition delay in the quadrupole echo was set to  $10T_1$  to allow for complete thermal relaxation. The preacquisition delays used ranged from 3 (360 K) to 75 s (260 K). Each FID was averaged from 1000 to 7400 times depending upon the temperature. Each FID was zero-filled to 8 K prior to Fourier transformation.

**UV-Visible Absorption.** Visible absorption spectra were measured using a Shimadzu UV-3100 spectrometer. For the measurement the monomer microcrystallites were pelletized with KBr. An 8-W UV lamp was used for the irradiation. The sample was positioned at a distance of 2 cm from the lamp. The measurements were conducted below ambient temperature.

**$\gamma$ -ray Irradiation.** In the first attempt we attempted to polymerize a sample of the Bis(14-2A)B monomer using  $^{60}\text{Co}$   $\gamma$ -rays with a dose rate of 1 Mrad  $\text{h}^{-1}$ . This method entails some sample heating, and the sample would have been heated

**Table 1.**  $^{13}\text{C}$  Solid-State Chemical Shifts and Spin-Lattice Relaxation Times ( $T_1$ ) of the Bis(14-2A)B Monomer at 298 K<sup>a</sup>

$^{13}\text{C}$ chemical shift (ppm)	assignment	$T_1$ (s)
14.7	14-CH <sub>3</sub>	2.7
24.1	13-CH <sub>2</sub>	5.0
29.6	2-CH <sub>2</sub>	5.6
30.6	3-CH <sub>2</sub>	5.3
32.0–33.3 <sup>a</sup>	4-CH <sub>2</sub> to 12-CH <sub>2</sub>	4.9, 5.1
20.6	1-CH <sub>2</sub>	5.2
66	$\delta$ -C	49
79	$\gamma$ -C	42
76	$\beta$ -C	49
88	$\alpha$ -C	37
123.2	aromatic-C	29
—	aromatic-CH	—

<sup>a</sup> The spin-lattice relaxation measurements were conducted under CP conditions. The atom numbering scheme is defined in Figure 1. <sup>b</sup> These resonances give two separate peaks in the solid-state  $^{13}\text{C}$  spectrum.

to above ambient. Later, (see the Discussion section) polymerization using  $\gamma$ -ray irradiation was again attempted but keeping the sample at 273 K (i.e., on ice).

## Results

**Differential Scanning Calorimetry.** Two scans from 133 to 450 K were performed on the monomer. At 300.6 K there was a sharp peak (lower boundary, 300.3 K; upper boundary 303.2 K, temperature width at half-height, 1.8 K;  $\Delta H$ ,  $-100 \pm 10$  kJ mol<sup>-1</sup>). This peak corresponded to the crystalline to plastic-crystalline phase transition. The sample melted at 376.2 K (lower boundary, 371.9 K; upper boundary, 378.2 K; temperature width at half-height, 1.8 K;  $\Delta H$   $-330 \pm 33$  kJ mol<sup>-1</sup>).

**$^{13}\text{C}$  NMR.** A  $^1\text{H}$ -decoupled  $^{13}\text{C}$  spectrum of Bis(14-2A)B dissolved in  $\text{CDCl}_3$  was assigned using our NMR spectral database system (SDBS-NMR).<sup>31,32</sup> This was used as the basis for assigning the  $^{13}\text{C}$  CP-MAS spectra of the molecule. The spectral assignments for the CP-MAS spectra are tabulated in Table 1 together with the corresponding spin-lattice relaxation times.

**Variable-Temperature  $^{13}\text{C}$  NMR Spectra of the Monomer.** The absence of characteristic color change for generating PDA and the similarity in chemical shift positions of the acetylenic carbons in the solid-state CP-MAS spectra after either 200 Mrad  $\gamma$ -ray irradiation at above 300 K or thermal treatment up to 343 K indicated that no significant polymerization had occurred. However, temperature-dependent changes were noticed in the CP-MAS spectra. Some representative CP-MAS spectra at various temperatures are given in Figure 2. The  $^{13}\text{C}$  chemical shifts of the four types of acetylene carbons moved to lower frequency with increasing temperature. The smallest and largest changes were observed for the  $\alpha$ - and  $\delta$ -acetylenic carbon resonances, respectively. Also, at 273 K the acetylenic resonances have shoulders on the lower frequency side. These shoulders move with temperature and move to the higher frequency side by 298 K. At 328 K they are not visible but reappear by 343 K on the higher frequency side. At 298 K the aliphatic resonances in the solid-state spectrum are similar to those of the solution spectrum, while below 298 K the aliphatic resonances at about 33 ppm appear as a single resonance with a small shoulder. This behavior is not observed in the solution spectra. The line widths of the aromatic carbon resonances are significantly reduced with increasing temperature. In addition, the aromatic CH resonances

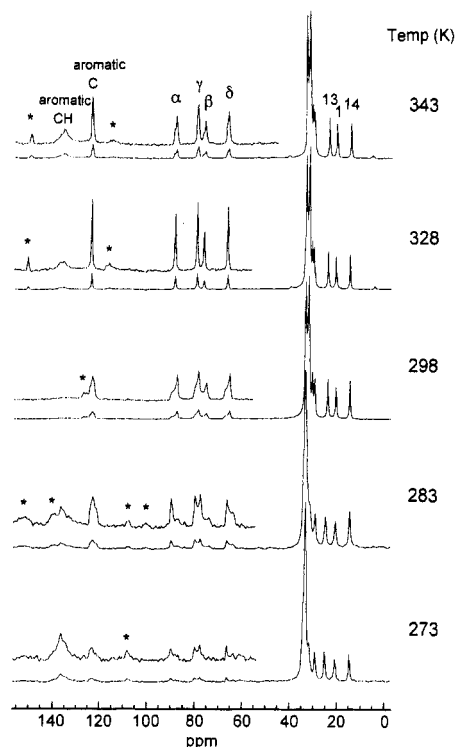


**Figure 2.**  $^{13}\text{C}$  CP-MAS spectra at various temperatures of Bis(14-2A)B. Asterisks denote spinning side bands or background signals. Significant temperature-dependent spectral changes are noted. At 273 K the aromatic CH resonances are clearly visible and the acetylenic resonances have significant shoulders. However, as the temperature increases, the aromatic CH resonances go through an intensity minimum at around 298 K. The shoulder patterns of the acetylenic resonances move from higher to lower frequencies as the temperature is increased. The aliphatic resonances at about 33 ppm, while appearing as a single line with a shoulder below 298 K, split into numerous lines above this temperature.

went through an intensity minimum at around 298 K (see Figure 2). The effects of temperature on the spectrum were reversible.

**$^{13}\text{C}$  NMR Spectra after  $\gamma$ -ray Irradiation at 273 K.** After making the above solid-state  $^{13}\text{C}$  NMR observations of the thermally treated and  $\gamma$ -ray irradiated monomer and correlating these results with the solid-state  $^2\text{H}$  NMR spectra of the deuterated monomer (see below and also the Discussion section), it was found that the monomer could be polymerized if the  $\gamma$ -ray irradiation was performed with the monomer being kept at low temperature. A CP-MAS spectrum of the monomer-polymer mixture after 120 Mrad of  $\gamma$ -ray irradiation at 273 K is given in Figure 3. The chemical shift assignments are summarized in Table 2. Some initial assignments were made by comparing the monomer-polymer spectrum with the monomer spectrum (i.e., Figure 2). Further assignments were made by comparing the  $^{13}\text{C}$  CP-MAS spectrum of the monomer-polymer mixture with the corresponding  $^{13}\text{C}$  CP-MAS/DD spectrum and inversion recovery spectra obtained with two different  $\tau$  delays (see Figure 4). The assignment procedure is further explained in the Discussion section. The polymerization yield was determined by comparing the integrated intensities of the monomer and polymer peaks in the  $^{13}\text{C}$  CP-MAS spectrum. High doses of  $\gamma$ -rays may induce some reactions of the methylene groups in the side chains. However, in the present work, such reactions could not be detected from the  $^{13}\text{C}$  NMR spectra.

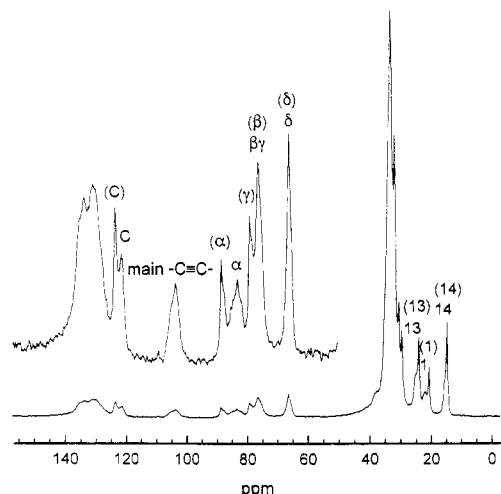


**Figure 3.**  $^{13}\text{C}$  CP-MAS spectrum at 298 K of the monomer-polymer mixture after 120 Mrad of  $\gamma$ -ray irradiation at 273 K. Comparison of this spectrum with that of the monomer only (see Figure 2) shows the addition of a number of additional peaks which are attributable to the formation of the polymer. Some assignments are given on the spectrum. The assignments in parentheses correspond to the monomer, and those without braces correspond to the polymer. "C" represents quaternary carbon.

**Table 2.**  $^{13}\text{C}$  Solid-State Chemical Shifts of Poly(Bis(14-2A)B) at 298 K<sup>a</sup>

$^{13}\text{C}$ chemical shift (ppm)	assignment	$^{13}\text{C}$ chemical shift (ppm)	assignment
15.5 <sup>c</sup>	14-CH <sub>3</sub>	77	$\beta$ -C
25 <sup>c</sup>	13-CH <sub>2</sub>	83	$\alpha$ -C
29.7	2-CH <sub>2</sub>	105	main chain -C≡C-
30.7	3-CH <sub>2</sub>	122	aromatic-C ( <i>para</i> )
32-35 <sup>b</sup>	4-CH <sub>2</sub> to 12-CH <sub>2</sub>	130	aromatic-CH ( <i>ortho</i> )
22 <sup>c</sup>	1-CH <sub>2</sub>	132	main chain -C=
66	$\delta$ -C	134	aromatic-CH ( <i>meta</i> )
77	$\gamma$ -C	136	aromatic-C

<sup>a</sup> The atom numbering scheme is according to the precursor monomers (see Figure 1) and the polymer (see Figure 7 orientation 1). <sup>b</sup> These resonances were not resolved in the solid-state spectrum. <sup>c</sup> Broad.

**$^2\text{H}$  NMR.**  $^2\text{H}$  NMR spectra of the  $^2\text{H}$ -labeled monomer were acquired for a number of temperatures in the range of 260–360 K. The experimental spectra were simulated using a program written in C++. The program included corrections for echo distortions, finite pulse power, virtual FID, and exchange during the radio-frequency pulses.<sup>34–36</sup> The program also included the ability to calculate log Gaussian distributions of flip rates<sup>37</sup> and various small-angle librational motions of the C–D bond.<sup>34</sup> We used the simplest model that would fit the observed spectra. It was found that the data could be well simulated using simple  $\pi$  flips characterized by a single correlation time ( $\tau_c$ ) of the deuterated phenyl ring. That the experimental spectra were able to be simulated using a simple  $\pi$  flip model means that any librational motions of the C–D bond must be quite small. It was found to be unnecessary to correct for the effects of the virtual FID. Some representative experimental spectra together with their respective simulations are given in Figure 5. The quadrupolar coupling constant was determined to be 175.5 kHz from the "static" pattern obtained at 260 K. This value is well within the range of 155–190 kHz commonly observed for *ortho* and *meta* deuterons.<sup>38</sup> While the local environment of the deuterium nuclei is almost certainly not axially symmetric, the quadrupolar asymmetry parameter ( $\eta$ ) is known to be very small<sup>38</sup>

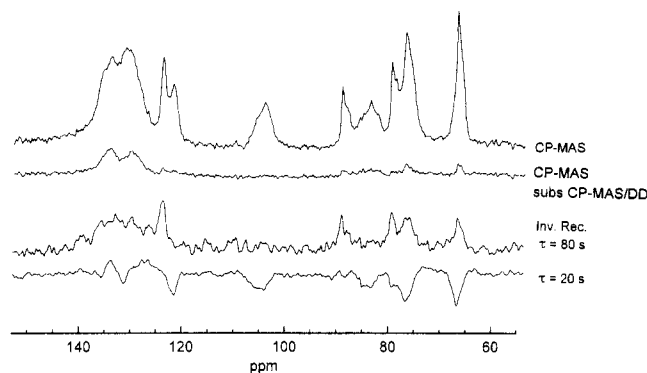


**Figure 4.**  $^{13}\text{C}$  CP-MAS (top line), difference between the CP-MAS and the corresponding CP-MAS/DD spectrum (second from top), and  $^{13}\text{C}$  inversion-recovery spectra acquired with a  $\tau$  delay of 80 (second from bottom) and 20 s (bottom), respectively. Only the nonaliphatic carbon regions of each spectrum are shown. The CP-MAS spectra contain resonances from all the carbon peaks of the monomer and the polymer, while the CP-MAS/DD spectrum only contains resonances from quaternary and mobile carbons. The difference spectrum contains only the aromatic CH carbons, while the inversion-recovery experiment shows mainly polymer signals when  $\tau = 20$  s and monomer signals when  $\tau = 80$  s. All measurements were performed at 298 K.

and mainly used out of cosmetic convenience;<sup>39</sup> hence, the simulations were performed with  $\eta$  set to 0. Other parameters used in the simulations are given in the caption to Figure 5. Below 260 K and above 360 K the observed  $^2\text{H}$  spectra approached the slow ( $\tau_c > 10^{-1}$  Hz<sup>-1</sup>) and fast exchange ( $\tau_c < 10^{-7}$  Hz<sup>-1</sup>) limits, respectively. Between 304 and 350 K there were noticeable changes in the fine structure, and after correcting for differences in the number of scans and the Boltzmann distribution, a large temperature dependence in the integrated spectral intensities was found. Below 304 K and above 350 K the integrated spectral intensities approached unity. The change in spectral intensity with temperature was used as a guide in simulating the experimental spectra. A plot of  $\ln(\tau_c)$  versus inverse temperature is given in Figure 6. Linear regression onto the data from 304 K and above gave the activation energy for the  $\pi$  flip to be  $60 \pm 1$  kJ mol<sup>-1</sup>.

**UV-Visible Absorption and Polymer Yield.** The Bis(14-2A)B monomer polymerized very slowly with UV irradiation at about 296 K. First, the broad absorption maximum around 685 nm appeared. The absorption edge was observed around 760 nm, and there was a shoulder around 600–640 nm. Further irradiation increased the absorbance of the maximum at 685 nm, and the shoulder changed to a maximum at 605 nm. After 4 h, the absorbances of the two maxima became almost the same; after 8 h there was not much further change in the spectrum and the color of the sample had become blue. Since the UV irradiation is not uniform throughout the KBr-pelletized sample, it is not possible to measure the actual polymer yield.

The Bis(14-2A)B sample irradiated by  $\gamma$ -rays also became blue, and the spectrum exhibited broad absorption from around 800 nm to cover all of the visible region. The maximum was around 550–600 nm and was shifted to shorter wavelength than that for the UV-irradiated samples. The polymer yield was determined gravimetrically (i.e., by the ratio of the benzene-insoluble part of the sample) to be 40%. The results of gel permeation chromatography of the benzene-soluble

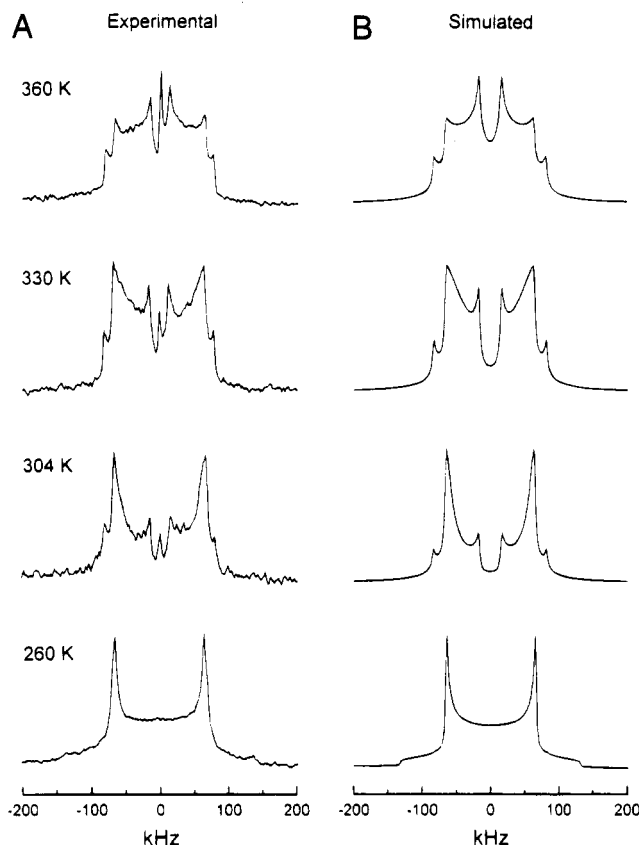


**Figure 5.** (A) Experimental and (B) simulated  $^2\text{H}$  NMR spectra of the Bis(14-2A)B monomer at various temperatures. The parameters used in the simulations were quadrupolar coupling constant 175.5 kHz,  $\eta = 0$ . The values of  $\tau_c$  used at the respective temperatures were  $1.0 \times 10^{-2} \text{ Hz}^{-1}$  (260 K),  $1.1 \times 10^{-4} \text{ Hz}^{-1}$  (304 K),  $1.8 \times 10^{-5} \text{ Hz}^{-1}$  (330 K),  $2.8 \times 10^{-6} \text{ Hz}^{-1}$  (360 K). The simulated spectra were calculated using  $1^\circ$  increments of the azimuthal and polar angles. The experimental spectra are presented with 2 kHz of Lorentzian line broadening. The simulated spectra are presented with 2 kHz of Lorentzian line broadening and 0.5 kHz of Gaussian line broadening. The peaks at zero frequency in the experimental spectra are artifacts.

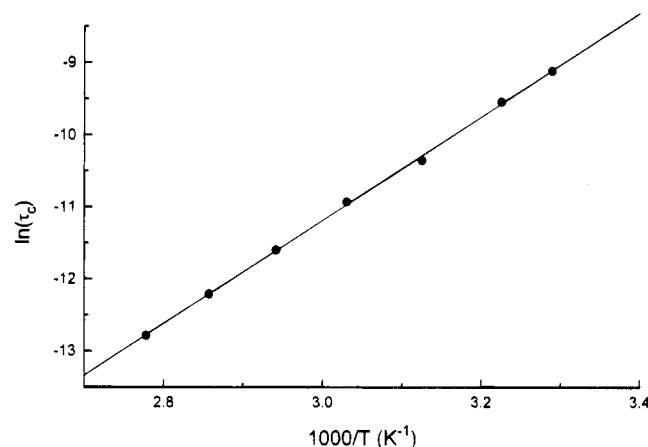


**Figure 6.** Plot of  $\ln(\tau_c)$  versus inverse temperature. The solid line represents regression of the formula,  $\tau_c = \tau_0 \exp(E_A/kT)$  onto the data. The points below 304 K were excluded from the calculation. The energy of activation ( $E_A$ ) for the flipping motion of the phenyl ring was determined to be  $60 \pm 1 \text{ kJ mol}^{-1}$  with  $\tau_0 = 6.5 \times 10^{-15} \text{ Hz}^{-1}$ .

part of the sample suggest the production of a small amount of oligomers. Since the remaining polymer is not soluble in conventional organic solvents, the molecular weight of the polymer could not be measured.

## Discussion

The appearance of fine structure in the 304 K  $^2\text{H}$  NMR spectrum, indicating the change from "rigid" phenyl rings to  $\pi$ -flipping phenyl rings, was in agreement with the observation of a phase change in the DSC measurement at 301 K. Thus, this phase change corresponds to the onset of rotational motion of the sp-bonded phenyl ring moiety around the long axis of the monomer molecule. Particularly notable is that ring flipping rarely occurs in crystalline compounds in which the ring is tied down at both ends.<sup>39</sup> The value of  $60 \pm 1 \text{ kJ mol}^{-1}$  obtained for the apparent activation energy for the pure  $\pi$  flip is a reasonably large value. Previously determined values for the activation energy have ranged from the theoretically determined value of  $25 \text{ kJ mol}^{-1}$  for poly(ethylene terephthalate)<sup>40</sup> to the experimentally determined value of  $47\text{--}58 \text{ kJ mol}^{-1}$  in *p*-fluoro-D,L-phenylalanine.<sup>38</sup> The relative signal-to-noise of the  $^{13}\text{C}$  resonances of the aromatic CH carbons went through a minimum around room temperature in the CP-MAS spectra. This diminution of intensity is indicative of increased molecular motion.<sup>23,24</sup> This observation is consistent with the presence of  $\pi$  flips of the phenyl ring. Similarly the narrowing of the resonances with temperature indicates increased molecular motion. The small changes in  $^{13}\text{C}$  chemical shift with temperature indicate that, apart from the  $\pi$ -flipping of the phenyl moiety, there was only a slight alteration in the average conformation of the monomer. The small changes in chemical shift between the solution and solid states and the ability to simulate the  $^2\text{H}$  NMR spectra without resorting to large librational angles of the  $\pi$  flip axis imply that the molecule remains quite linear, at least in the vicinity of the phenyl moiety. From the high activation energy for the  $\pi$  flip it can be inferred that large steric forces prevent easy rotation of the monomer. The high melting point is, as noted in the DSC measurement, probably correlated with the alkyl chains being "stuck" together by van der Waals forces and thus further preventing molecular motion.

The solid-state  $^{13}\text{C}$  chemical shifts of the monomer at 298 K were all at higher frequency than those of the corresponding solution-state resonances; larger differences between solution- and solid-state chemical shifts were noted for the aliphatic resonances near the acetylenic groups. This is consistent with large van der Waals forces between the chains inducing tight packing of the alkyl chains in the solid state.<sup>41</sup> The small shoulders noted for the acetylenic carbons in the  $^{13}\text{C}$  CP-MAS spectra (see Figure 2) indicate a small degree of polymorphism of the monomer in the solid state. This effect has been noted previously in solid-state spectra of similar compounds.<sup>41,42</sup> In a study of PDA's with directly bound aromatics, both polymerizable and non-polymerizable polymorphs of the monomers were found.<sup>43</sup> Although the  $^{13}\text{C}$  CP-MAS spectra indicate a small degree of polymorphism, the  $^2\text{H}$  NMR spectra were able to be simulated using only one mode of motion of the phenyl ring. Thus, the phenyl ring motion is the same in all of the statistically significant polymorphs. Particularly informative of the temperature-dependent conformational processes were the aliphatic resonances at about 33 ppm (see Figure 2). Below about 298 K these resonances appeared as a single line with a small shoulder, above this temperature the resonance and shoulder split into a number of peaks. This change coincides closely with the phase change observed in the DSC measurement (N.B. the temperature control in the

CP-MAS experiment is likely to be a few degrees in error) and the onset of (observable)  $\pi$ -flipping of the phenyl ring. This splitting (downfield shift) of the resonances is thus indicative of a loss of alignment (i.e., loss of stacking) and change in segmental motions of the aliphatic chains with increasing temperature.<sup>44</sup> The small changes with temperature of the resonance for atoms 1, 13, and 14 but the larger changes for the carbon resonances in the middle of the aliphatic chain imply that it is the central part of the aliphatic chain that is important in the stacking process. In agreement with the small temperature effect on the resonance for first carbon atom of the aliphatic chain the  $\delta$ -acetylenic carbon resonance has a very small chemical shift change with temperature. The  $\alpha$ -acetylenic carbon resonance has a much larger shift with temperature which indicates a large change in its environment with the changing motion of the phenyl ring with temperature. It is not possible, however to determine if it is the looser packing of the alkyl chains at higher temperatures that allows the rotation of the phenyl ring or whether the loss of alignment results from the increased steric "pressure" caused by the rotating phenyl rings.

At room temperature the longest  $^{13}\text{C}$   $T_1$  relaxation times were found, as expected, for the acetylenic carbons with their  $T_1$  values ranging from 37 to 49 s; next came the aliphatic carbons with  $T_1$  values ranging from 4.9 to 5.6 s. The shortest relaxation time was found for the highly mobile terminal methyl group (N.B. the reorientational motion of the molecule is outside the extreme narrowing condition). The dominant  $^{13}\text{C}$  NMR relaxation mechanism for carbons is the dipole-dipole mechanism, and thus the quaternary acetylenic carbons have longer relaxation times due to the absence of any directly bonded protons.

The results of the absorption spectroscopy also show that the polymerization of the Bis(14-2A)B monomer occurs very slowly. As is discussed below, it is clear that the solid-state polymerization results with the monomers having the relative positions as shown in orientation 1 in Figure 7. The experimental evidence suggests that the reason that the monomer fails to polymerize using thermal treatment up to 343 K or  $\gamma$ -ray irradiation at temperatures above 300 K (N.B.  $\gamma$ -irradiation causes a significant increase in the sample temperature) is that above 300 K the alkyl chains of the monomers are no longer sufficiently aligned for the 1,4-addition mechanism to proceed. Similarly, it has been noted that phospholipids containing diacetylene groups polymerize more readily when the monomer is cooled below the lipid transition temperature.<sup>45</sup> A further experiment was performed in which the monomer was irradiated with  $\gamma$ -rays at 273 K by keeping the sample on ice. The polymer conversion of more than  $75 \pm 5\%$  was first estimated from the integrated intensities of the monomer and polymer resonances in the  $^{13}\text{C}$  CP-MAS spectrum (see Figure 3). However, the yield obtained by the gravimetric method was only 40%. This large difference between the two methods results mainly from not all  $^{13}\text{C}$  nuclei having the same cross-polarization efficiency. Also, small amounts of soluble oligomers may also result in a decrease in the gravimetrically determined polymer yield. The value determined by the gravimetric method is more reliable than that determined by NMR. Since the polymer yield for  $\gamma$ -ray irradiation is generally higher than that for UV irradiation, the polymer backbone structure in the  $\gamma$ -irradiated sample must be distorted due to the large

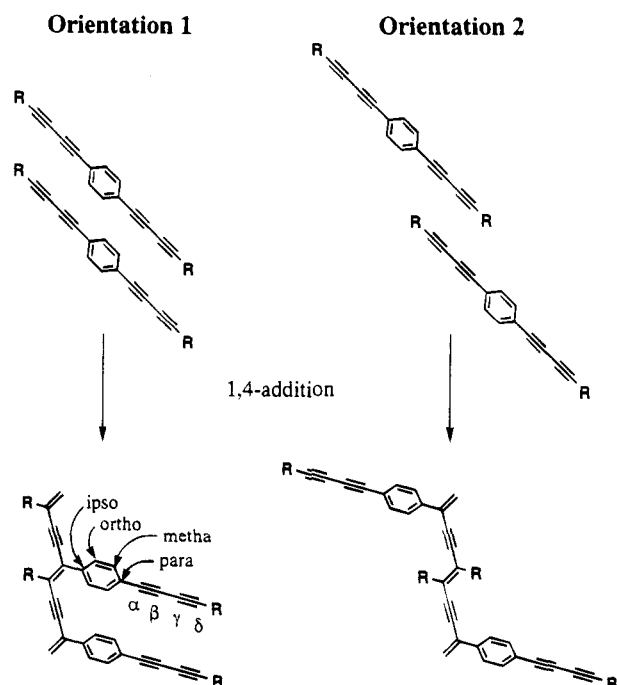


**Figure 7.** Solid-state polymerization of the Bis(14-2A)B monomer. The polymerization occurs via the 1,4-addition mechanism. The structure of the resulting polymer depends on the relative orientation between any two reacting monomers. Our results imply that the polymerization occurs with the monomers having the alignment shown in orientation 1. R represents the  $\text{C}_{14}\text{H}_{29}$  alkyl chain.

movement of substituents in the course of polymerization, resulting in the shift of the absorption maximum to shorter wavelengths for the  $\gamma$ -irradiated sample. Similar absorption shifts due to differences in polymer conversion have been observed in other diacetylenes including tetraynes.<sup>46,47</sup>

The polymer assignments in the  $^{13}\text{C}$  spectrum were made in the first instance by comparing the monomer-polymer spectrum with the monomer spectrum. In almost all cases the polymer resonances were considerably broader than the corresponding monomer resonances due to the slower molecular reorientation of the polymer. For example, compare the resonances of the terminal methyl groups of the monomer (14.8 ppm) and polymer (15.5 ppm). Further assignment was possible by comparing the CP-MAS spectrum with the corresponding CP-MAS/DD spectrum. The CP-MAS/DD spectrum only measures quaternary and mobile carbons. The difference spectrum obtained by subtracting the CP-MAS/DD spectrum from the CP-MAS spectrum allowed the assignment of the polymer *ortho* and *meta* aromatic CH resonances. By comparing the inversion-recovery spectra acquired with different  $\tau$  delays, some monomer resonances could be distinguished from the polymer resonances on the basis of the slower relaxation time of the polymer (see Figure 4). From this comparison the polymer main chain  $-\text{C}=\text{C}-$  and aromatic  $-\text{C}=\text{C}-$  were able to be assigned. From the CP-MAS spectrum (and the assignments in Tables 1 and 2) it can be seen that upon polymerization the chemical shifts of the newly polymerized monomer resonances shift to lower field.

Particularly indicative of polymer formation was the totally new peak at 105 ppm which was assigned to the acetylene group in the main-chain and the aromatic CH peaks splitting into separate resonances for the *ortho* and *meta* positions. As schematically presented in



Figure 7, it is clear that a different polymer will result depending on the initial relative orientation of the monomer units prior to polymerization. We must now consider which of the two possibilities is consistent with our experimental data. The coincidence of the beginning of the phenyl ring flipping and the loss of alkyl chain alignment at around the same temperature implies that the two phenomena are correlated. This is consistent with the monomer units having orientation 1 (see Figure 7). A further pointer to orientation 1, and not orientation 2, being the dominant orientation prior to polymerization is that van der Waals forces are more likely to be effective in orientation 1 where full alignment of the alkyl chains is possible.

In poly(Bis(14-2A)B) structure (see orientation 1 in Figure 7) the two main-chain olefinic carbons (i.e.,  $>C=$ ) are not chemically equivalent; however, there is little difference in the observed chemical shift (we cannot distinguish between the two in the  $^{13}C$  CP-MAS spectrum; see Figure 3 and Table 2). However, in poly(14-4A) there was a chemical shift difference of more than 35 ppm between the corresponding olefinic carbons.<sup>19</sup> Thus, it appears that the conjugation effect is not as strong in the current polymer.

## Conclusions

The experimental data discussed above are consistent with the monomer molecules in the crystal state being reasonably rigid and aligned below the crystalline to plastic-crystalline phase transition point. Above this transition point the alignment of the aliphatic chains is, to some degree, lost. The data suggest that the loss of alignment occurs at the onset of the flipping motion of the phenyl ring. Alignment of the monomers is known to be a prerequisite for the 1,4-addition, and because this condition is not met, neither thermal treatment nor  $\gamma$ -ray irradiation at 298 K is successful in initiating polymerization. This led to the devising of novel polymerization conditions (i.e., low-temperature  $\gamma$ -ray irradiation) that allowed the monomer to successfully polymerize. Thus, polymerization occurs more readily when the monomer and polymer phases are more alike. The study clearly shows that an understanding of the fundamental dynamic and mechanical properties of molecules in crystals is prerequisite to devising suitable synthetic pathways in solid-state reactions.

## References and Notes

- Brédas, J. L.; Adant, C.; Tackx, P.; Persoons, A. *Chem. Rev.* **1994**, *94*, 243.
- Sauteret, C.; Hermann, J.-P.; Frey, R.; Pradère, F.; Dueuing, J.; Baughman, R. H.; Chance, R. R. *Phys. Rev. Lett.* **1976**, *36*, 956.
- Etemad, S.; Soos, Z. G. In *Spectroscopy of Advanced Materials*, Clark, R. J. H., Hester, R. E. Eds.; Wiley: New York, 1991; p 87.
- Etemad, S.; Baker, G. L.; Soos, Z. G. In *Molecular Nonlinear Optics: Materials, Physics, and Devices*, Zyss, J., Ed.; Academic Press: Boston, 1994; p 433.
- Kajzar, F.; Messier, J.; Zyss, J.; Ledoux, I. *Opt. Commun.* **1983**, *45*, 113.
- Carter, G. M.; Hryniewicz, J. V.; Thakur, M. K.; Chen, Y.; Maylor, S. E. *Appl. Phys. Lett.* **1986**, *49*, 998.
- Hattori, T.; Kobayashi, T. *Chem. Phys. Lett.* **1987**, *133*, 230.
- Wegner, G. *Z. Naturforsch.* **1969**, *24B*, 824.
- Nakanishi, H.; Matsuda, H.; Okada, S.; Kato, M. *Springer Proc. Phys.* **1989**, *36*, p 155.
- Okada, S.; Matsuda, H.; Nakanishi, H.; Kato, M.; Otsuka, M. *Thin Solid Films* **1989**, *179*, 423.
- Okada, S.; Matsuda, H.; Nakanishi, H.; Kato, M. *Mol. Cryst. Liq. Cryst.* **1990**, *189*, 57.
- Okada, S.; Ohsugi, M.; Masaki, A.; Matsuda, H.; Takaragi, S.; Nakanishi, H. *Mol. Cryst. Liq. Cryst.* **1990**, *183*, 81.
- Okada, S.; Matsuda, H.; Masaki, A.; Nakanishi, H.; Hayamizu, K. *Chem. Lett.* **1990**, 2213.
- Hayamizu, K.; Okada, S.; Tsuzuki, S.; Matsuda, H.; Masaki, A.; Nakanishi, H. *Bull. Chem. Soc. Jpn.* **1994**, *67*, 342.
- Enkelmann, V. *Makromol. Chem.* **1982**, *109-110*, 253.
- Mayerle, J. J.; Flandrera, M. A. *Acta Crystallogr.* **1978**, *B34*, 1374.
- Baughman, R. H. *J. Polym. Sci., Polym. Phys. Ed.* **1974**, *12*, 1511.
- Nakanishi, H.; Matsuda, H.; Okada, S.; Kato, M. *Fr. Macromol. Sci.* **1988**, 469.
- Okada, S.; Hayamizu, K.; Matsuda, H.; Masaki, A.; Nakanishi, H. *Bull. Chem. Soc. Jpn.* **1991**, *64*, 857.
- Matsuda, H.; Nakanishi, H.; Minami, N.; Kato, M. *Mol. Cryst. Liq. Cryst.* **1988**, *160*, 241.
- Okada, S.; Doi, T.; Kikuchi, N.; Hayamizu, K.; Matsuda, H.; Nakanishi, H. *Mol. Cryst. Liq. Cryst.* **1994**, *247*, 99.
- Okada, S.; Matsuda, H.; Otsuka, M.; Nakanishi, H.; Kato, M. *Bull. Chem. Soc. Jpn.* **1994**, *67*, 483.
- VanderHart, D. L.; Earl, W. L.; Garroway, A. N. *J. Magn. Reson.* **1981**, *44*, 361.
- Jarret, W. L.; Mathias, L. J.; Alamo, R. G.; Mandelkern, L.; Dorset, D. L. *Macromolecules* **1992**, *25*, 3468.
- Rice, D. M.; Wittebort, R. J.; Griffin, R. J.; Meirovitch, E.; Stimson, E. R.; Meinwald, Y. C.; Freed, J. H.; Scheraga, H. A. *J. Am. Chem. Soc.* **1981**, *103*, 7707.
- Cholli, A. L.; Dumais, J. J.; Engel, A. K.; Jelinski, L. W. *Macromolecules* **1984**, *17*, 2399.
- Sonogashira, K.; Tohda, Y.; Hagihara, N. *Tetrahedron Lett.* **1975**, 4467.
- Takahashi, S.; Kuroyama, Y.; Sonogashira, K.; Hagihara, N. *Synthesis* **1980**, 627.
- Ishikawa, N.; Sekiya, A. *Bull. Chem. Soc. Jpn.* **1974**, *47*, 1680.
- Torchia, D. A. *J. Magn. Reson.* **1978**, *30*, 613.
- Yamamoto, O.; Hayamizu, K.; Yanigasawa, M. *Anal. Sci.* **1988**, *4*, 461.
- Yamamoto, O.; Hayamizu, K.; Yanigasawa, M. *Anal. Sci.* **1989**, *5*, 645.
- Price, W. S.; Hayamizu, K. *J. Magn. Reson. A* **1995**, *114*, 73.
- Greenfield, M. S.; Ronemus, A. D.; Vold, R. L.; Vold, R. R.; Ellis, P. D.; Raidy, T. E. *J. Magn. Reson.* **1987**, *72*, 89.
- Barbara, T. M.; Greenfield, M. S.; Vold, R. L.; Vold, R. R. *J. Magn. Reson.* **1986**, *69*, 311.
- Bloom, M.; Davis, J. H.; Valic, M. *Can. J. Phys.* **1980**, *58*, 1510.
- Wehrle, M.; Hellman, G. P.; Spiess, H. W. *Colloid Polym. Sci.* **1987**, *265*, 815.
- Hiyama, Y.; Silverton, J. V.; Torchia, D. A.; Gerig, J. T.; Hammond, S. J. *J. Am. Chem. Soc.* **1986**, *108*, 2715.
- Henrichs, P. M.; Luss, H. R.; Scaringe, R. P. *Macromolecules* **1989**, *22*, 2731.
- Tonelli, A. E. *J. Polym. Sci., Polym. Lett. Ed.* **1973**, *11*, 441.
- Okada, S.; Hayamizu, K.; Matsuda, H.; Masaki, A.; Minami, N.; Nakanishi, H. *Macromolecules* **1994**, *27*, 6259.
- Okada, S.; Matsuda, H.; Masaki, A.; Nakanishi, H.; Hayamizu, K. In *Nonlinear Optical Properties of Organic Materials IV*; Singer, K. D., Ed.; Proceedings of SPIE 1560; SPIE: Bellingham, WA, 1991; p 25.
- Ohsugi, M.; Takaragi, S.; Matsuda, H.; Okada, S.; Masaki, A.; Nakanishi, H. In *Nonlinear Optical Properties of Organic Materials III*; Khanarian, G., Ed.; Proceedings of SPIE 1337; SPIE: Bellingham, WA, 1990; p 162.
- Hayamizu, K.; Okada, S.; Doi, T.; Kawanami, H.; Kikuchi, N.; Matsuda, H.; Nakanishi, H. *Bull. Chem. Soc. Jpn.* **1995**, *68*, 791.
- Johnston, D. S.; Sanghera, S.; Pons, M.; Chapman, D. *Biochim. Biophys. Acta* **1980**, *602*, 57.
- Tieke, B.; Lieser, G. J. *J. Colloid Interface Sci.* **1982**, *88*, 471.
- Okada, S.; Matsuda, H.; Masaki, A.; Nakanishi, H.; Hayamizu, K. *Mater. Res. Soc. Symp. Proc.* **1991**, *214*, 29.

MA950167Q